
Plan-R1: Safe and Feasible Trajectory Planning as Language Modeling

Xiaolong Tang Meina Kan Shiguang Shan Xilin Chen
Institute of Computing Technology, Chinese Academy of Sciences
University of Chinese Academy of Sciences
tangxiaolong22s@ict.ac.cn

Abstract

Safe and feasible trajectory planning is essential for real-world autonomous driving systems. However, existing learning-based planning methods often rely on expert demonstrations, which not only lack explicit safety awareness but also risk inheriting unsafe behaviors such as speeding from suboptimal human driving data. Inspired by the success of large language models, we propose Plan-R1, a novel two-stage trajectory planning framework that formulates trajectory planning as a sequential prediction task, guided by explicit planning principles such as safety, comfort, and traffic rule compliance. In the first stage, we train an autoregressive trajectory predictor via next motion token prediction on expert data. In the second stage, we design rule-based rewards (e.g., collision avoidance, speed limits) and fine-tune the model using Group Relative Policy Optimization (GRPO), a reinforcement learning strategy, to align its predictions with these planning principles. Experiments on the nuPlan benchmark demonstrate that our Plan-R1 significantly improves planning safety and feasibility, achieving state-of-the-art performance. Our code will be made public soon.

1 Introduction

Trajectory planning is a fundamental component of autonomous driving systems, directly influencing vehicle safety, efficiency, and the ability to navigate complex and dynamic environments. In recent years, learning-based planning approaches have attracted increasing attention due to their strong adaptability, competitive performance, and minimal reliance on manually designed rules. These methods offer promising solutions for generating high-quality context-sensitive trajectories that can respond effectively to various traffic scenarios and rapidly changing road conditions.

However, due to the complexity of large-scale real-world datasets such as nuPlan [2], most existing planning methods, whether based on imitation learning [4, 5, 8, 11, 17, 37, 40] or reinforcement learning [9, 12, 15, 38], rely heavily on expert demonstrations for supervision. This dependency introduces two key limitations. First, expert data often lacks negative scenarios (e.g., collisions, off-road driving), making it difficult for models to learn explicit safety constraints such as maintaining drivable area compliance or avoiding collisions. Second, expert demonstrations are not always optimal and may contain unsafe behaviors. For example, we find that approximately 11.2% of the nuPlan training scenes exhibit speeding, and some contain uncomfortable maneuvers or critically low time-to-collision (TTC) values. Models trained directly on such data risk inheriting these undesirable behaviors without a clear notion of safety or feasibility.

To address these limitations, we draw inspiration from the success of large language models (LLMs) [22, 30], which typically follow a two-stage training paradigm. LLMs are first trained as a general-purpose predictor via self-supervised pretraining, and then fine-tuned using reinforcement learning from human feedback (RLHF) to align outputs with human preferences. Our key

insight is that trajectory planning can similarly be formulated as a two-stage training process, i.e., first trained as a sequence prediction model on expert driving data, and then fine-tuned using reinforcement learning to align the planning behavior with explicit planning principles, such as safety, comfort, and rule compliance. This decoupled paradigm separates behavior learning and planning principle alignment, enabling the system to retain valuable driving behaviors while discarding unsafe patterns learned from the expert data.

Specifically, our proposed Plan-R1 method consists of two sequential stages. In the pre-training stage, the trajectories are discretized into motion tokens across time and space following prior studies [24, 29, 36], and an autoregressive model is trained via next motion token prediction. In the fine-tuning stage, the pre-trained model is frozen as a reactive world model to predict the motions of surrounding agents, while a duplicate copy is fine-tuned for ego trajectory planning. These two models collaboratively perform multi-step predictions to generate the joint future of the ego vehicle and surrounding agents. To guide fine-tuning, we design interpretable, rule-based reward functions that evaluate various aspects of planned trajectories, including but not limited to on-road adherence, collision avoidance, speed limit compliance, and driving comfort. The ego planner is then fine-tuned using Generalized Reinforcement Policy Optimization (GRPO) [30] algorithm with these rewards. Experiments on the nuPlan benchmark demonstrate that Plan-R1 significantly enhances planning safety and feasibility, achieving state-of-the-art (SOTA) performance.

The primary contributions of this paper are:

- We propose a new perspective that formulates trajectory planning as a principle-aligned sequence prediction task, enabling the decoupling of behavior learning and planning principle alignment.
- We introduce Plan-R1, a two-stage trajectory planning framework that combines autoregressive pre-training with reinforcement learning fine-tuning to align with planning principles.
- Instead of relying on preference data for fine-tuning, a set of interpretable, rule-based reward functions is designed to capture essential planning principles, including but not limited to drivable area compliance, collision avoidance, speed limit compliance, and driving comfort.
- Our Plan-R1 significantly improves the safety and feasibility of planned trajectories, achieving SOTA performance on the nuPlan benchmark, particularly outperforming existing planners in the reactive closed-loop simulation setting.

2 Related Work

2.1 Learning-based trajectory planning

Learning-based trajectory planning methods for autonomous driving can be broadly categorized into imitation learning (IL) and reinforcement learning (RL). IL trains policies to imitate expert behavior, typically using large-scale datasets of human driving trajectories, and has been shown to produce realistic, human-like motion in complex urban environments [1, 4, 5, 25, 27, 35]. RL, on the other hand, optimizes policies through interaction with the environment to maximize task-specific rewards, enabling the discovery of behaviors beyond those observed in demonstrations [9, 12, 15, 16, 38].

Despite promising results in simulation, both IL and RL face key limitations when applied to real-world planning. IL is fundamentally constrained by the quality and coverage of expert demonstrations. RL methods, while more flexible, often address the challenges of complex reward design and sample inefficiency by using the negative distance to expert trajectories as the reward function [15, 38], thereby remaining dependent on expert data. However, expert trajectories are not always safe or optimal, and models trained on such data may inherit undesirable behaviors, such as traffic violations or infeasible maneuvers. Our key insight is that explicitly decoupling behavior learning from planning principle alignment can help mitigate this issue—a direction largely overlooked in prior IL- and RL-based planners.

2.2 Trajectory generation as language modeling

Inspired by the success of LLMs, recent studies have explored formulating trajectory generation as a sequence modeling task. These approaches [24, 29, 36] discretize agent trajectories into motion tokens and train autoregressive models via next motion token prediction. This formulation allows

the model to learn the multi-modal distribution of driving behaviors from demonstrations and has shown strong performance in trajectory prediction and simulation. However, most of these methods focus exclusively on the pre-training stage, overlooking the fine-tuning phase that is now standard in modern LLM pipelines, such as RLHF in InstructGPT [22]. While these models can produce diverse and plausible trajectories, they often lack guarantees of safety, feasibility, or rule compliance during execution. Our work bridges this gap by introducing reinforcement learning-based fine-tuning to align generated trajectories with explicit planning principles, analogous to how LLMs are aligned with human preference, but tailored to safety-critical planning.

Concurrent work TrajHF [15] and earlier Gen-Drive [12] both align planning behavior with human preferences via reinforcement learning from human feedback (RLHF). In contrast to our use of interpretable rule-based rewards derived from domain knowledge, these methods depend heavily on preference data. TrajHF minimizes the distance to expert-annotated preferred trajectories, while Gen-Drive trains a reward model from pairwise comparisons to guide learning. Both face two key limitations: collecting high-quality preferences is costly and labor-intensive, and performance is highly sensitive to data quality and coverage, limiting generalization beyond the annotated distribution.

2.3 Reinforcement learning algorithms for sequence-level fine-tuning

Recent progress in LLMs has demonstrated the effectiveness of reinforcement learning algorithms in aligning sequence generation with desired objectives. In particular, Proximal Policy Optimization (PPO) [28] has emerged as the practical choice for RLHF, and has been widely adopted for fine-tuning LLMs such as InstructGPT [22]. More recently, GRPO [30] has been proposed as a lightweight alternative that eliminates the need for value functions by computing relative advantages within a group of sampled sequences. Compared to PPO, GRPO simplifies implementation by removing the value critic, reducing memory overhead, and avoiding instability caused by inaccurate value estimates. GRPO has demonstrated strong performance across various LLM tasks involving search [10, 18] and reasoning [13, 23]. Motivated by the sequential nature of trajectory generation, which closely parallels text generation, we adopt GRPO to fine-tune our planning model. Our experiments demonstrate that this formulation enables reinforcement learning to effectively align motion sequence generation with high-level planning principles.

3 Method

We propose Plan-R1, a two-stage framework that decouples behavior learning and planning principle alignment to improve trajectory safety and feasibility. As illustrated in Figure 1, Plan-R1 consists of an autoregressive pre-training stage and a reinforcement learning fine-tuning stage. The model is first trained on expert demonstrations to learn multimodal motion behaviors, and then fine-tuned with rule-based rewards to align the ego vehicle’s behavior with explicit planning principles. In Section 3.1, we present our formulation of trajectory planning as a principle-aligned sequence generation task. In Section 3.2, we describe the autoregressive pre-training process on expert data. Finally, in Section 3.3, we detail how fine-tuning is performed via the GRPO algorithm with trajectory-level rewards.

3.1 Problem formulation

Trajectory generation is inherently sequential, which makes autoregressive modeling a natural and effective choice for this task. Building on this formulation, we further incorporate alignment with high-level planning principles such as safety, comfort, and traffic rule compliance. Concretely, we reformulate trajectory planning as a principle-aligned autoregressive generation task. In this formulation, the ego vehicle’s trajectory is generated jointly with the predicted motions of surrounding agents [3, 7, 39], enabling the planner to account for multi-agent interactions and ensure safe, feasible planning. Specifically, given a scene context C —including current and historical observations, map information, and navigation routes—and a set of planning principles P , the goal is to generate the joint future trajectories for all agents:

$$Y = f(C, P), \quad Y = \{y_{t,n}\}_{t \in [1:F], n \in [0:N]}, \quad (1)$$

where agent 0 is ego, N denotes the number of surrounding agents and F is the planning horizon. Directly modeling the joint distribution $p(Y | C, P)$ is intractable due to its high dimensionality.

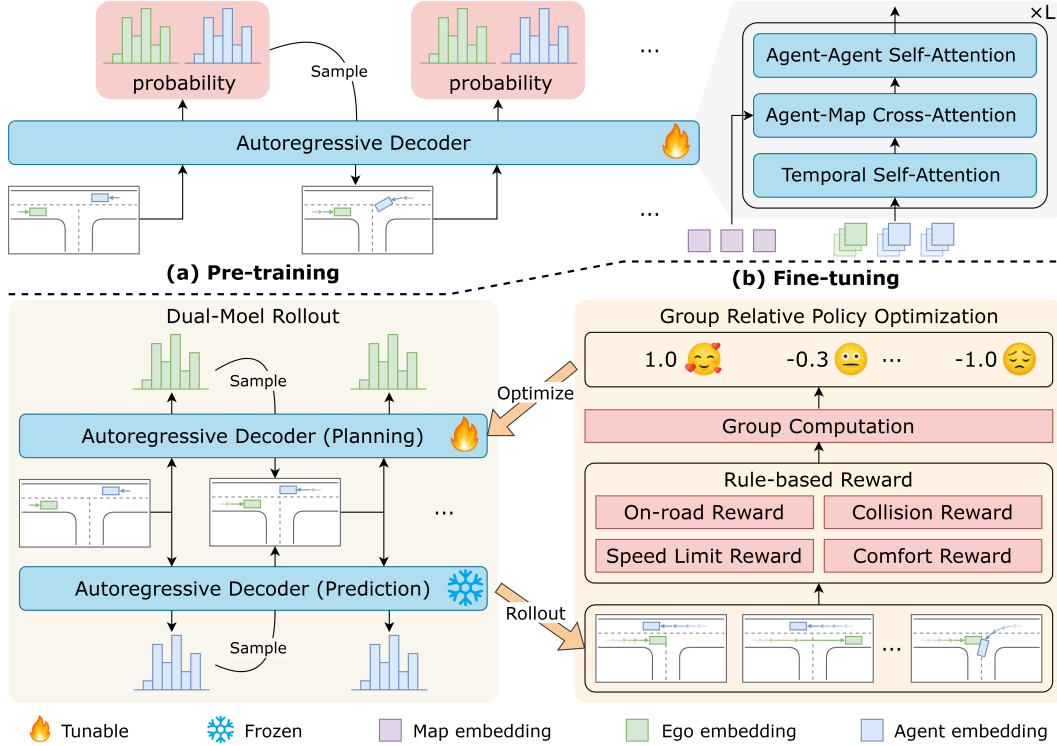


Figure 1: Illustration of our two-stage Plan-R1. In the pre-training stage, an autoregressive model is trained via next motion token prediction on expert data. In the fine-tuning stage, the model is optimized using the GRPO algorithm with rule-based rewards to align the generated trajectories with planning principles such as safety, feasibility, and comfort.

However, by leveraging temporal causality [29] and the short-term conditional independence between agents [26, 32], the joint distribution can be factorized as:

$$\begin{aligned}
 p(Y | C, P) &= \prod_{t=1}^F p(y_{t,0:N} | y_{<t,0:N}, C, P) \\
 &= \prod_{t=1}^F p(y_{t,0} | y_{<t,0:N}, C, P) \prod_{n=1}^N p(y_{t,n} | y_{<t,0:N}, C, P) \\
 &\approx \prod_{t=1}^F \pi_e(y_{t,0} | y_{<t,0:N}, C, P) \prod_{n=1}^N p_a(y_{t,n} | y_{<t,0:N}, C),
 \end{aligned} \tag{2}$$

where the final line reflects that the behaviors of surrounding agents are independent of the ego’s planning principles. This decomposition yields two sub-problems: (i) $p_a(y_{t,n} | y_{<t,0:N}, C)$, predicting each surrounding agent’s motion conditioned on the joint history and scene context, and (ii) $\pi_e(y_{t,0} | y_{<t,0:N}, C, P)$, generating the ego trajectory with additional conditioning on planning principles. The distribution p_a is naturally modeled as an autoregressive sequence prediction task, in which the future motion of each agent is inferred from its own history and the history of surrounding agents, along with the scene context. π_e introduces additional constraints on the ego trajectory to meet planning principles such as safety, comfort, and rule compliance. Since p_a is trained on human driving data, which inherently follows these planning principles, it captures a range of plausible and realistic behaviors. Therefore, we assume that p_a provides a reasonable prior for π_e . However, p_a lacks explicit alignment with these planning objectives, and its generated trajectories may still violate safety constraints or result in suboptimal decisions in complex scenarios, rendering it unsuitable for direct deployment in safety-critical planning tasks. To address this, we initialize π_e with p_a , then fine-tune π_e using reinforcement learning with rule-based rewards to explicitly align the ego’s behavior with the planning principles.

3.2 Autoregressive pre-training

Tokenization. To facilitate sequence modeling, continuous trajectories are discretized into motion tokens. Temporally, trajectories are segmented at fixed intervals. Spatially, the K-disk clustering algorithm [24] is applied to the resulting motion segments based on their average corner distance, producing a motion token vocabulary. Each token represents a prototypical displacement and heading trajectory over a fixed time step. For each agent, the entire trajectory is thus transformed into a sequence of such motion tokens spanning the prediction horizon.

Model architecture. Our model employs a transformer decoder with factorized attention [20, 21] to encode multi-agent spatiotemporal interactions, as shown in Figure 1 (a). It is designed to capture the temporal dynamics of each agent’s trajectory and its interactions with the map and nearby agents.

Following prior work [29, 36], the model processes motion tokens through a stack of attention-based fusion blocks at each time step. Each block sequentially applies three key components: temporal self-attention, agent-map cross-attention, and agent-agent cross-attention. Temporal self-attention models the motion continuity of an individual agent over time, enabling the model to capture temporal dependencies in the agent’s trajectory. Agent-map cross-attention incorporates spatial constraints by attending to relevant road elements, guiding trajectories to comply with the road network. Finally, agent-agent cross-attention captures local interactions among neighboring agents within a fixed distance threshold, enabling the model to reason about agent interactions in dynamic environments.

To preserve translation invariance and rotation invariance, relative spatiotemporal position embedding [33, 42] is applied to all attention modules. The ego and non-ego agents share the same encoder structure, and all attention computations are performed in a query-centric manner to support efficient multi-agent rollout.

Training objective. The model is trained with a next motion token prediction objective. Given a tokenized trajectory sequence, the model is trained to minimize the negative log-likelihood of the next motion token at each step:

$$\mathcal{L}_{pretrain} = - \sum_{t=1}^F \sum_{n=0}^N \log p_a(a_{t,n} | a_{<t,0:N}, C), \tag{3}$$

where $a_{t,n}$ is the motion token of agent i at time t . This objective allows the model to approximate the latent distribution of human driving behaviors, capturing diverse and realistic motion patterns as demonstrated in large-scale expert data. Notably, no explicit planning principles are introduced at this stage; the model purely imitates human-like behavior conditioned on the scene context.

3.3 Reinforcement learning fine-tuning

While autoregressive pre-training captures human-like motion patterns, it does not explicitly enforce adherence to planning principles. This is particularly problematic when expert trajectories include undesirable behaviors—e.g., speeding or uncomfortable maneuvers—which may be inadvertently retained during pretraining. To mitigate this issue, we fine-tune the ego trajectory generator using reinforcement learning, as shown in Figure 1 (b), optimizing it to align with predefined planning principles. The generation process is framed as a sequential decision-making problem, where the ego agent selects motion tokens to maximize rewards that reflect desirable planning behaviors.

Dual-Model rollout. To enable stable multi-agent rollout and principle-aligned fine-tuning, we adopt a dual-model design. Specifically, we freeze the pretrained autoregressive model for predicting the future motions of the surrounding agents, and create a trainable replica to represent the ego policy π_e . During each rollout, the two models jointly generate trajectories step by step. The frozen model, serving as a reactive world model, predicts the future motions of surrounding agents based on the history of all agents, including the ego. Although fixed during training, the world model remains responsive to ego actions by updating its predictions based on the ego’s historical motion tokens. This interaction ensures that the surrounding agents’ behaviors are aligned with the ego vehicle’s actions, ensuring realistic, interaction-aware simulation in multi-agent settings. Meanwhile, the trainable ego model explores alternative actions and receives feedback through the reward function. This separation enables ego-centric policy updates without destabilizing surrounding agent dynamics, while also ensuring that all agents exhibit natural reactive behaviors, as observed in real-world interactions.

Rule-based rewards. To align the ego policy with planning principles, we design a set of interpretable, rule-based reward functions. Rewards are computed based on the final predicted trajectories and are designed to reflect key planning properties such as safety, feasibility, and comfort. Following [2, 9], we compute the total reward as the product of two components: a set of multiplicative safety indicators (e.g., driving area compliance) and a weighted sum of soft cost terms (e.g., comfort):

$$R(Y) = \prod_{k \in \mathcal{I}_{\text{safe}}} \mathbf{1}_k \cdot \sum_{j \in \mathcal{I}_{\text{cost}}} w_j \cdot r_j(Y), \quad (4)$$

where $\mathbf{1}_k \in \{0, 1\}$ denotes whether safety constraint k is satisfied, and $r_j(Y)$ is the score of cost term j with weight w_j . This formulation ensures that violations of critical safety conditions will nullify the total reward, while soft planning objectives are optimized when safety constraints are satisfied. Details of the reward components and implementation are provided in the Appendix A.2.

Optimization with GRPO. To fine-tune the ego policy toward planning principles, we adopt GRPO as our reinforcement learning algorithm. Compared to PPO, GRPO eliminates the need for an explicit value function by computing relative advantages within sampled trajectory groups. This reduces implementation complexity, avoids the instability associated with inaccurate value estimates, and improves sampling efficiency, making it well-suited for trajectory-level planning.

During fine-tuning, we treat the pre-trained trajectory predictor as the reference policy π_{ref} , and the ego trajectory generator as the trainable policy π_e . For each scenario, GRPO samples a group of joint future trajectories $\{Y_1, Y_2, \dots, Y_G\}$ from the old policy π_{old} , where each sample contains both ego and nearby agents’ predicted trajectories. The trainable policy π_e is updated by minimizing this loss:

$$\mathcal{L}_{\text{finetune}} = -\frac{1}{G} \sum_{g=1}^G \left(\frac{\pi_e(Y_g | C, P)}{\pi_{\text{old}}(Y_g | C, P)} \hat{A}_g - \beta D_{\text{KL}}[\pi_e \| \pi_{\text{ref}}] \right), \quad (5)$$

where \hat{A}_g is the normalized relative advantage of the g -th joint future Y_g within the sampled group. $\hat{A}_g = (R(Y_g) - \mu_R) / \sigma_R$, where μ_R, σ_R are the mean and standard deviation of the group’s reward values, respectively. This group-wise normalization eliminates the need for a learned value critic, allowing stable optimization through relative comparison across trajectories in the same rollout batch.

The KL divergence term in the loss serves as a regularizer, constraining the updated policy π_e to remain close to the reference policy π_{ref} . This helps preserve the prior learned during pretraining, preventing the fine-tuned policy from deviating too far from reasonable behaviors.

4 Experiments

4.1 Experimental setup

Datasets. We evaluate our method on the nuPlan [2] benchmark, a large-scale platform designed for trajectory planning in autonomous driving. The dataset contains over 1,300 hours of expert driving logs collected across four cities, covering diverse real-world scenarios, such as merges, intersections, roundabouts, lane changes, and interactions with pedestrians. The benchmark supports simulation-based evaluation, where scenarios are replayed for 15 seconds at 10 Hz. The ego vehicle executes planned trajectories via a bicycle model and an LQR controller, while other traffic agents follow either replayed or Intelligent Driver Model (IDM) [34] policies. Following PLUTO [4], we sample 1M training instances across all scenario types for autoregressive pretraining. To reduce the computational cost of closed-loop rollouts during reinforcement learning, we construct a smaller dataset of 100,000 scenarios for fine-tuning. Evaluations are conducted on the standard Val14 [6], Test14-random, and Test14-hard [5] splits under both non-reactive and reactive simulation settings.

Metrics. We evaluate planning performance in closed-loop simulation using the Non-Reactive Closed-Loop Score (NR-CLS) and Reactive Closed-Loop Score (R-CLS). These metrics assess the planner’s ability to generate safe and feasible trajectories over 15-second rollouts, considering collisions, off-road driving, speed limit violations, and the progress of the expert route. In the NR-CLS setting, surrounding agents follow replayed logged trajectories, while in R-CLS, they react using the IDM [34] planner. Each score ranges from 0 to 100, where a higher score indicates better performance.

Table 1: Comparison with SOTAs on nuPlan benchmark. The best result is in **bold** and the second best result is underlined. *: with rule-based post-processing. NR/R: non-reactive/reactive mode.

Type	Planner	Val14		Test14-hard		Test14-random	
		NR	R	NR	R	NR	R
Expert	Log-Replay	93.53	80.32	85.96	68.80	94.03	75.86
Rule-based & Hybrid	IDM [34]	75.60	77.33	56.15	62.26	70.39	72.42
	PDM-Closed* [6]	92.84	92.12	65.08	75.19	90.05	91.64
	PDM-Hybrid* [6]	92.77	92.11	65.99	76.07	90.10	91.28
	Gameformer* [11]	79.94	79.78	68.70	67.05	83.88	82.05
	PLUTO* [4]	92.88	89.84	80.08	76.88	92.23	90.29
	PlanAgent* [41]	93.26	92.75	72.51	76.82	-	-
	Diffusion Planner* [40]	<u>94.26</u>	<u>92.90</u>	<u>78.87</u>	82.00	94.80	<u>91.75</u>
	Carplanner* [38]	-	-	-	-	94.07	91.10
	Plan-R1* (Ours)	94.77	93.25	77.79	<u>80.97</u>	<u>94.11</u>	94.51
Learning-based	UrbanDriver [27]	68.57	64.11	50.40	49.95	51.83	67.15
	PDM-Open [6]	53.53	54.24	33.51	35.83	52.81	57.23
	PlanTF [5]	84.27	76.95	69.70	61.61	85.62	79.58
	PLUTO [4]	<u>88.89</u>	78.11	70.03	59.74	89.90	78.62
	Diffusion Planner [40]	89.87	<u>82.80</u>	75.99	<u>69.22</u>	89.19	<u>82.93</u>
	Plan-R1 (Ours)	87.99	84.97	<u>75.31</u>	73.18	<u>89.46</u>	88.89

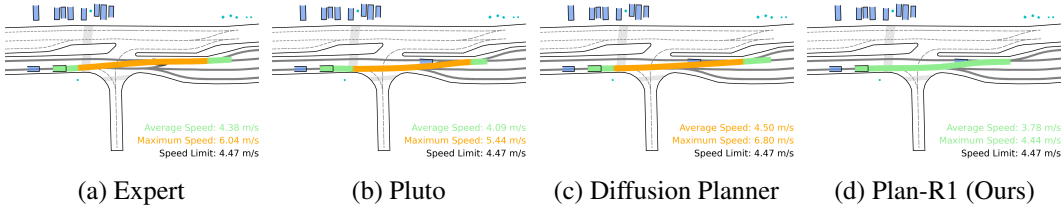


Figure 2: Comparison of closed-loop ego trajectories in a non-reactive scenario without post-processing. Trajectories are color-coded: orange marks speeding segments, while green indicates compliant motion. The expert trajectory (a) contains a clear speeding segment, replicated by both PLUTO (b) and Diffusion Planner (c), showing that the planners based on expert data inherit undesirable behaviors therein. In contrast, Plan-R1 (d) avoids speeding, demonstrating the effectiveness of reinforcement learning fine-tuning in promoting safety-compliant behavior.

4.2 Comparison with SOTAs

Quantitative results. We compare our method, Plan-R1, against a wide range of existing planners on the nuPlan benchmark, as shown in Table 1. Across all three benchmarks, Plan-R1 achieves performance comparable to the strongest prior method, Diffusion Planner [40], under the non-reactive setting. This indicates that our reinforcement learning fine-tuning preserves the model’s ability to align with expert-like behavior. Under the more challenging reactive setting, where surrounding agents respond dynamically to the ego vehicle, Plan-R1 substantially outperforms all baselines. It achieves state-of-the-art reactive scores of 84.97 on Val14, 73.18 on Test14-hard, and 94.51 on Test14-random, surpassing the next-best method, Diffusion Planner, by +2.17, +3.96, and +5.96 points, respectively. Compared to other learning-based planners such as PlanTF [5], Plan-R1 demonstrates significantly stronger generalization to interactive scenarios. We attribute this improvement to the exploration capability introduced by reinforcement learning, which enables the planner to generate safer and more feasible trajectories beyond what is directly covered in the expert demonstrations. Following Diffusion Planner [40], we apply the existing refinement module [31] as a post-processing step to Plan-R1, ensuring a fair comparison with prior methods that adopt similar pipelines. With post-processing, Plan-R1 continues to achieve state-of-the-art performance, reaching a reactive score of 94.51 on Test14-random, outperforming the second-best method by 2.76 points. This result highlights the effectiveness of our approach in producing high-quality trajectories.

Table 2: The importance of the fine-tuning stage.

Planner	Score	Collisions	TTC	Drivable	Speed	Comfort	Progress
Baseline (w/o finetning)	82.81	94.44	90.04	94.64	97.83	99.62	85.71
Plan-R1 (w/ finetning)	88.89	96.55	94.25	97.70	99.46	99.46	88.69
Δ	+6.08	+2.11	+4.21	+3.06	+1.63	-0.16	+2.98

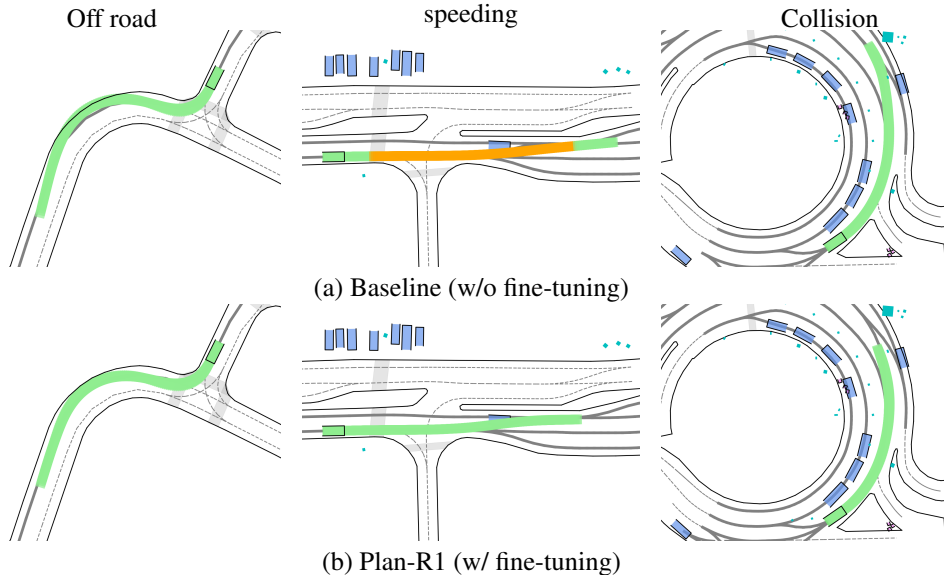


Figure 3: Comparison of closed-loop ego trajectories generated by the baseline (a) and Plan-R1 (b) in three non-reactive closed-loop simulation scenarios. The baseline exhibits issues such as off-road driving (left), speeding (middle), and collision with static obstacles (right), while Plan-R1 avoids these issues, generating safe and feasible trajectories. **orange** indicates segments where the ego exceeds the local speed limit, while **cyan** indicates static obstacles.

We attribute these gains to our two-stage training framework: autoregressive pretraining establishes a strong behavioral prior from expert data, while reinforcement learning fine-tuning explicitly aligns trajectory generation with safety and feasibility objectives. Together, these stages enable Plan-R1 to produce safe, feasible, and socially compliant behaviors in closed-loop planning scenarios.

Qualitative Results. To further illustrate the practical benefits of our approach, we conduct a case study comparing closed-loop non-reactive rollouts across different planners on a representative scenario from the nuPlan dataset. In this scenario, the expert trajectory exhibits a speeding behavior that violates the local speed limit. We evaluate three learning-based planners—PLUTO [4], Diffusion Planner [40], and Plan-R1—none of which incorporate rule-based post-processing in this analysis. As shown in Figure 2, both PLUTO and Diffusion Planner, which are trained solely via supervised learning on expert demonstrations, replicate the speeding behavior in their closed-loop rollouts. In contrast, Plan-R1 successfully avoids speeding and maintains a compliant velocity profile throughout the rollout. This demonstrates our model’s ability to identify and correct undesirable behaviors inherited from expert data, a capability enabled by reinforcement learning fine-tuning with rule-based reward supervision. These results highlight the importance of explicit objective alignment in ensuring rule-compliant and safe planning behavior.

4.3 Ablation studies

The importance of the fine-tuning stage. To evaluate the effectiveness of the fine-tuning stage in our Plan-R1 framework, we compare Plan-R1 with a baseline model that undergoes only pretraining, as shown in Table 2. Compared to the baseline without fine-tuning, Plan-R1 shows substantial improvements across key metrics in the reactive closed-loop simulation on Test14-random. Specifically,

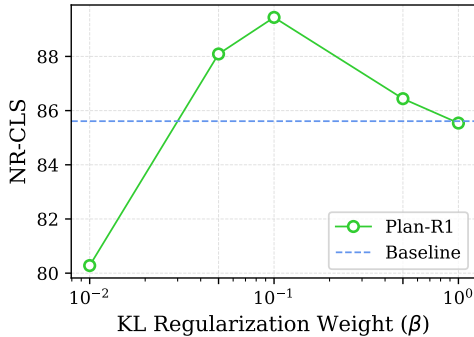


Figure 4: Effect of KL regularization weight on NR-CLS. A moderate KL weight ($\beta=0.1$) achieves the best performance.

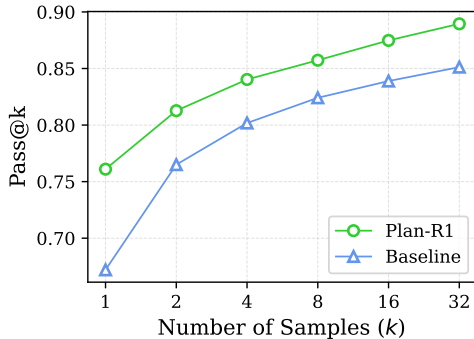


Figure 5: Comparison of pass@ k between the pretrained baseline and Plan-R1. Plan-R1 always achieves higher pass@ k .

it achieves a score increase of +6.08, with notable gains in collision avoidance (+2.11), time-to-collision (TTC) (+4.21), drivable area compliance (+3.06), and speed limit compliance (+1.63). Although the comfort score fluctuated slightly (-0.16), the progress score improved significantly (+2.98), suggesting that the model enhances safety and feasibility not by relying on remaining stationary or abrupt braking, but by generating better trajectories.

To further illustrate the benefits of fine-tuning, we compare the closed-loop ego trajectories from the baseline and Plan-R1 in three non-reactive scenarios. As shown in Figure 3, the baseline exhibits off-road driving, speeding, and collision with an obstacle, respectively. In contrast, Plan-R1 avoids these issues, producing trajectories that adhere to the road, obey speed limits, and avoid obstacles. These results highlight the crucial role of fine-tuning in improving planning safety and feasibility.

Effect of KL regularization. We investigate the impact of the KL divergence regularization weight β in Equation (5) during the fine-tuning stage. As shown in Figure 4, when β is set too small (e.g., 0.01), the updated policy deviates excessively from the pretrained reference, leading to a degradation in performance due to the loss of learned motion priors. Conversely, when β is too large (e.g., 1.0), the policy is overly constrained to remain close to the reference model, limiting the benefits of fine-tuning and resulting in similar results. A moderate value (e.g., $\beta=0.1$) achieves the best balance, preserving the distributional prior while enabling meaningful adaptation toward planning objectives.

Pass@ k analysis. To further assess the reliability of our method under varying sampling conditions, we conduct a pass@ k [14] analysis on the validation set. For both the pretrained baseline and our Plan-R1, we generate k trajectories per scenario and compute the proportion of cases where at least one satisfies all core safety and feasibility criteria—i.e., staying within drivable areas, avoiding collisions, respecting speed limits, and maintaining comfort. As shown in Figure 5, pass@ k improves with increasing k for both models. However, Plan-R1 consistently outperforms the baseline, indicating it yields high-quality trajectories with greater likelihood. This suggests that fine-tuning not only improves the single-shot performance but also enhances the model’s ability to generate feasible trajectories across multiple samples, which is critical for robust planning under uncertainty.

5 Conclusion

In this work, we introduced Plan-R1, a novel two-stage framework for safe and feasible trajectory planning. Inspired by the success of LLMs, we reformulate trajectory planning as a principle-aligned sequence generation task, decoupling behavior learning from planning principle alignment. Specifically, we first pretrain an autoregressive model to capture the multimodal distribution of expert demonstrations, and then fine-tune the ego policy using reinforcement learning guided by interpretable, rule-based rewards. Experiments on the nuPlan benchmark demonstrate that Plan-R1 achieves SOTA performance, especially in the reactive simulation. Our results underscore the effectiveness of aligning planning trajectory with safety and feasibility objectives through reinforcement learning.

References

- [1] Mayank Bansal, Alex Krizhevsky, and Abhijit Ogale. Chauffeurnet: Learning to drive by imitating the best and synthesizing the worst. *arXiv preprint arXiv:1812.03079*, 2018.
- [2] Holger Caesar, Juraj Kabzan, Kok Seang Tan, Whye Kit Fong, Eric Wolff, Alex Lang, Luke Fletcher, Oscar Beijbom, and Sammy Omari. nuplan: A closed-loop ml-based planning benchmark for autonomous vehicles. *arXiv preprint arXiv:2106.11810*, 2021.
- [3] Zhili Chen, Maosheng Ye, Shuangjie Xu, Tongyi Cao, and Qifeng Chen. Ppad: Iterative interactions of prediction and planning for end-to-end autonomous driving. In *Proceedings of the European Conference on Computer Vision (ECCV)*, 2024.
- [4] Jie Cheng, Yingbing Chen, and Qifeng Chen. Pluto: Pushing the limit of imitation learning-based planning for autonomous driving. *arXiv preprint arXiv:2404.14327*, 2024.
- [5] Jie Cheng, Yingbing Chen, Xiaodong Mei, Bowen Yang, Bo Li, and Ming Liu. Rethinking imitation-based planners for autonomous driving. In *IEEE International Conference on Robotics and Automation (ICRA)*, 2024.
- [6] Daniel Dauner, Marcel Hallgarten, Andreas Geiger, and Kashyap Chitta. Parting with misconceptions about learning-based vehicle motion planning. In *Conference on Robot Learning (CoRL)*, 2023.
- [7] Steffen Hagedorn, Marcel Hallgarten, Martin Stoll, and Alexandru Paul Condurache. The integration of prediction and planning in deep learning automated driving systems: A review. *IEEE Transactions on Intelligent Vehicles*, 2024.
- [8] Marcel Hallgarten, Martin Stoll, and Andreas Zell. From prediction to planning with goal conditioned lane graph traversals. In *IEEE International Conference on Intelligent Transportation Systems (ITSC)*, 2023.
- [9] Yihan Hu, Siqi Chai, Zhening Yang, Jingyu Qian, Kun Li, Wenxin Shao, Haichao Zhang, Wei Xu, and Qiang Liu. Solving motion planning tasks with a scalable generative model. In *Proceedings of the European Conference on Computer Vision (ECCV)*, 2024.
- [10] Wenxuan Huang, Bohan Jia, Zijie Zhai, Shaosheng Cao, Zheyu Ye, Fei Zhao, Zhe Xu, Yao Hu, and Shaohui Lin. Vision-r1: Incentivizing reasoning capability in multimodal large language models. *arXiv preprint arXiv:2503.06749*, 2025.
- [11] Zhiyu Huang, Haochen Liu, and Chen Lv. Gameformer: Game-theoretic modeling and learning of transformer-based interactive prediction and planning for autonomous driving. In *Proceedings of the IEEE/CVF International Conference on Computer Vision (ICCV)*, 2023.
- [12] Zhiyu Huang, Xinshuo Weng, Maximilian Igl, Yuxiao Chen, Yulong Cao, Boris Ivanovic, Marco Pavone, and Chen Lv. Gen-drive: Enhancing diffusion generative driving policies with reward modeling and reinforcement learning fine-tuning. *arXiv preprint arXiv:2410.05582*, 2024.
- [13] Bowen Jin, Hansi Zeng, Zhenrui Yue, Jinsung Yoon, Sercan Arik, Dong Wang, Hamed Zamani, and Jiawei Han. Search-r1: Training llms to reason and leverage search engines with reinforcement learning. *arXiv preprint arXiv:2503.09516*, 2025.
- [14] Sumith Kulal, Panupong Pasupat, Kartik Chandra, Mina Lee, Oded Padon, Alex Aiken, and Percy S Liang. Spoc: Search-based pseudocode to code. *Advances in Neural Information Processing Systems (NIPS)*, 2019.
- [15] Derun Li, Jianwei Ren, Yue Wang, Xin Wen, Pengxiang Li, Leimeng Xu, Kun Zhan, Zhongpu Xia, Peng Jia, Xianpeng Lang, et al. Finetuning generative trajectory model with reinforcement learning from human feedback. *arXiv preprint arXiv:2503.10434*, 2025.
- [16] Qifeng Li, Xiaosong Jia, Shaobo Wang, and Junchi Yan. Think2drive: Efficient reinforcement learning by thinking with latent world model for autonomous driving (in carla-v2). In *Proceedings of the European Conference on Computer Vision (ECCV)*, 2024.

- [17] Haochen Liu, Li Chen, Yu Qiao, Chen Lv, and Hongyang Li. Reasoning multi-agent behavioral topology for interactive autonomous driving. *arXiv preprint arXiv:2409.18031*, 2024.
- [18] Ziyu Liu, Zeyi Sun, Yuhang Zang, Xiaoyi Dong, Yuhang Cao, Haodong Duan, Dahua Lin, and Jiaqi Wang. Visual-rft: Visual reinforcement fine-tuning. *arXiv preprint arXiv:2503.01785*, 2025.
- [19] Ilya Loshchilov and Frank Hutter. Decoupled weight decay regularization. In *Proceedings of the International Conference on Learning Representations (ICLR)*, 2018.
- [20] Nigamaa Nayakanti, Rami Al-Rfou, Aurick Zhou, Kratarth Goel, Khaled S Refaat, and Benjamin Sapp. Wayformer: Motion forecasting via simple & efficient attention networks. In *IEEE International Conference on Robotics and Automation (ICRA)*, 2023.
- [21] Jiquan Ngiam, Vijay Vasudevan, Benjamin Caine, Zhengdong Zhang, Hao-Tien Lewis Chiang, Jeffrey Ling, Rebecca Roelofs, Alex Bewley, Chenxi Liu, Ashish Venugopal, et al. Scene transformer: A unified architecture for predicting future trajectories of multiple agents. In *Proceedings of the International Conference on Learning Representations (ICLR)*, 2021.
- [22] Long Ouyang, Jeffrey Wu, Xu Jiang, Diogo Almeida, Carroll Wainwright, Pamela Mishkin, Chong Zhang, Sandhini Agarwal, Katarina Slama, Alex Ray, et al. Training language models to follow instructions with human feedback. *Advances in Neural Information Processing Systems (NIPS)*, 2022.
- [23] Jiazhen Pan, Che Liu, Junde Wu, Fenglin Liu, Jiayuan Zhu, Hongwei Bran Li, Chen Chen, Cheng Ouyang, and Daniel Rueckert. Medvlm-r1: Incentivizing medical reasoning capability of vision-language models (vlms) via reinforcement learning. *arXiv preprint arXiv:2502.19634*, 2025.
- [24] Jonah Philion, Xue Bin Peng, and Sanja Fidler. Trajenglish: Learning the language of driving scenarios. *arXiv preprint arXiv:2312.04535*, 2023.
- [25] Stefano Pini, Christian S Perone, Aayush Ahuja, Ana Sofia Rufino Ferreira, Moritz Niendorf, and Sergey Zagoruyko. Safe real-world autonomous driving by learning to predict and plan with a mixture of experts. In *IEEE International Conference on Robotics and Automation (ICRA)*, 2023.
- [26] Nicholas Rhinehart, Rowan McAllister, Kris Kitani, and Sergey Levine. Precog: Prediction conditioned on goals in visual multi-agent settings. In *Proceedings of the IEEE/CVF International Conference on Computer Vision (ICCV)*, 2019.
- [27] Oliver Scheel, Luca Bergamini, Maciej Wolczyk, Błażej Osipiński, and Peter Ondruska. Urban driver: Learning to drive from real-world demonstrations using policy gradients. In *Conference on Robot Learning (CoRL)*, 2022.
- [28] John Schulman, Filip Wolski, Prafulla Dhariwal, Alec Radford, and Oleg Klimov. Proximal policy optimization algorithms. *arXiv preprint arXiv:1707.06347*, 2017.
- [29] Ari Seff, Brian Cera, Dian Chen, Mason Ng, Aurick Zhou, Nigamaa Nayakanti, Khaled S Refaat, Rami Al-Rfou, and Benjamin Sapp. Motionlm: Multi-agent motion forecasting as language modeling. In *Proceedings of the IEEE/CVF International Conference on Computer Vision (ICCV)*, 2023.
- [30] Zhihong Shao, Peiyi Wang, Qihao Zhu, Runxin Xu, Junxiao Song, Xiao Bi, Haowei Zhang, Mingchuan Zhang, YK Li, Y Wu, et al. Deepseekmath: Pushing the limits of mathematical reasoning in open language models. *arXiv preprint arXiv:2402.03300*, 2024.
- [31] Qiao Sun, Huimin Wang, Jiahao Zhan, Fan Nie, Xin Wen, Leimeng Xu, Kun Zhan, Peng Jia, Xianpeng Lang, and Hang Zhao. Generalizing motion planners with mixture of experts for autonomous driving. *arXiv preprint arXiv:2410.15774*, 2024.
- [32] Charlie Tang and Russ R Salakhutdinov. Multiple futures prediction. *Advances in Neural Information Processing Systems (NIPS)*, 2019.

- [33] Xiaolong Tang, Meina Kan, Shiguang Shan, Zhilong Ji, Jinfeng Bai, and Xilin Chen. Hpnet: Dynamic trajectory forecasting with historical prediction attention. In *Proceedings of the IEEE/CVF Conference on Computer Vision and Pattern Recognition (CVPR)*, 2024.
- [34] Martin Treiber, Ansgar Hennecke, and Dirk Helbing. Congested traffic states in empirical observations and microscopic simulations. *Physical review E*, 2000.
- [35] Matt Vitelli, Yan Chang, Yawei Ye, Ana Ferreira, Maciej Wolczyk, Błażej Osiński, Moritz Niendorf, Hugo Grimmett, Qiangui Huang, Ashesh Jain, et al. Safetynet: Safe planning for real-world self-driving vehicles using machine-learned policies. In *IEEE International Conference on Robotics and Automation (ICRA)*, 2022.
- [36] Wei Wu, Xiaoxin Feng, Ziyang Gao, and Yuheng Kan. Smart: scalable multi-agent real-time motion generation via next-token prediction. *Advances in Neural Information Processing Systems (NIPS)*, 2024.
- [37] Dongkun Zhang, Jiaming Liang, Sha Lu, Ke Guo, Qi Wang, Rong Xiong, Zhenwei Miao, and Yue Wang. Pep: Policy-embedded trajectory planning for autonomous driving. *IEEE Robotics and Automation Letters (RA-L)*, 2024.
- [38] Dongkun Zhang, Jiaming Liang, Ke Guo, Sha Lu, Qi Wang, Rong Xiong, Zhenwei Miao, and Yue Wang. Carplanner: Consistent auto-regressive trajectory planning for large-scale reinforcement learning in autonomous driving. *arXiv preprint arXiv:2502.19908*, 2025.
- [39] Wenzhao Zheng, Ruiqi Song, Xianda Guo, Chenming Zhang, and Long Chen. Genad: Generative end-to-end autonomous driving. In *Proceedings of the European Conference on Computer Vision (ECCV)*, 2024.
- [40] Yinan Zheng, Ruiming Liang, Kexin Zheng, Jinliang Zheng, Liyuan Mao, Jianxiong Li, Weihao Gu, Rui Ai, Shengbo Eben Li, Xianyuan Zhan, et al. Diffusion-based planning for autonomous driving with flexible guidance. *arXiv preprint arXiv:2501.15564*, 2025.
- [41] Yupeng Zheng, Zebin Xing, Qichao Zhang, Bu Jin, Pengfei Li, Yuhang Zheng, Zhongpu Xia, Kun Zhan, Xianpeng Lang, Yaran Chen, et al. Planagent: A multi-modal large language agent for closed-loop vehicle motion planning. *arXiv preprint arXiv:2406.01587*, 2024.
- [42] Zikang Zhou, Jianping Wang, Yung-Hui Li, and Yu-Kai Huang. Query-centric trajectory prediction. In *Proceedings of the IEEE/CVF Conference on Computer Vision and Pattern Recognition (CVPR)*, 2023.

A Technical Appendices and Supplementary Material

A.1 Additional ablation study: parameter scaling baseline

Since our Plan-R1 integrates a pretrained trajectory predictor and a fine-tuned planner, it potentially increases the overall parameter count. To assess whether the performance improvement of Plan-R1 stems purely from this increase in model capacity, we conduct an ablation study comparing it with a scaled-up baseline model. This scaled baseline increases the hidden dimension from 128 to 192, resulting in approximately doubling the number of parameters.

As shown in Table 3, the Baseline (2 \times) shows modest improvements over the original baseline in a few metrics, such as overall score (+2.13), collision avoidance (+1.15), and progress (+1.40). However, several critical metrics, including TTC, speed limit compliance, and comfort, do not improve with increased capacity; in fact, their performance slightly degrades (TTC: -0.38, Speed: -0.24, Comfort: -1.15). We attribute this phenomenon to the imperfections in the expert data, which contain suboptimal behaviors such as speeding, uncomfortable motion patterns, and overly short TTC. As the model capacity increases, the baseline becomes more capable of faithfully imitating these undesirable patterns, leading to the reproduction—and even amplification—of unsafe or uncomfortable behaviors in simulation.

In contrast, Plan-R1 achieves consistent and substantial improvements across almost all metrics. Compared to the Baseline (2 \times), it improves the overall score by +3.95 and achieves notable gains in TTC (+4.59), speed limit compliance (+1.87), and other safety-related metrics. These results indicate that Plan-R1 benefits not only from increased capacity, but more importantly from its structured design. In particular, the fine-tuning stage explicitly aligns generation with planning principles via rule-based rewards, mitigating undesirable behaviors inherited from expert data and improving safety awareness in trajectory generation.

Table 3: Comparison between the original baseline, a scaled-up baseline with approximately twice the parameter count (Baseline 2 \times), and Plan-R1.

Planner	Score	Collisions	TTC	Drivable	Speed	Comfort	Progress
Baseline	82.81	94.44	90.04	94.64	97.83	99.62	85.71
Baseline (2 \times)	84.94	95.59	89.66	95.79	97.59	98.47	87.11
Plan-R1	88.89	96.55	94.25	97.70	99.46	99.46	88.69

A.2 Reward design

We design the total reward as a product of two components: a set of binary safety indicators and a weighted sum of soft cost terms. This formulation first ensures that no reward is given if any critical safety condition is violated, and then encourages the agent to optimize for smoother and more efficient trajectories when safety is satisfied. Below, we describe the components in detail.

Safety indicators ($\mathcal{I}_{\text{safe}}$). The following constraints must all be satisfied to receive a non-zero reward:

- **Driving area compliance:** All predicted positions must lie within the drivable area polygon.
- **No collision with dynamic agents:** At each prediction step, the ego vehicle must not collide with the predicted positions of any surrounding agent at the corresponding time step.
- **No collision with static obstacles:** All predicted positions must avoid collisions with static obstacles.

To ensure accurate safety assessment, all collision checks are performed using the full bounding boxes of the ego vehicle and surrounding agents, rather than using center points.

Soft cost terms ($\mathcal{I}_{\text{cost}}$). When all safety indicators are satisfied, the agent receives a soft reward computed as a weighted sum of four normalized terms:

- **Comfort** ($w = 2$): This term penalizes high lateral and longitudinal accelerations, angular velocity, and angular acceleration. If any of these exceed predefined thresholds, the comfort score is set to 0; otherwise, it is 1.
- **Time-to-collision (TTC)** ($w = 4$): This term is set to 1 if the predicted TTC remains above a safety threshold throughout the trajectory; otherwise, it is set to 0.
- **Speed limit compliance** ($w = 5$): This term linearly penalizes the predicted speeding behavior by computing the ratio between the total over-speed distance and a predefined maximum over-speed threshold. The score decreases linearly from 1 to 0 as this ratio increases, following the same formulation as in the nuPlan benchmark [2].
- **Progress** ($w = 2$): This term measures the forward progress of the predicted trajectory along the reference route. It is normalized using the progress of the expert trajectory. The progress is computed by projecting each predicted position onto the centerline of the reference route and accumulating the forward distance along the projected path. Note that this is not an imitation loss: we do not minimize the distance between the predicted and expert trajectories, but only use the expert’s final progress as a normalization reference.

Each reward term $r_j(Y)$ is normalized to the range $[0, 1]$, and the overall soft reward is computed as a weighted sum $\sum_{j \in \mathcal{I}_{\text{cost}}} w_j \cdot r_j(Y)$. This design encourages smooth, efficient, and rule-compliant trajectories, while ensuring that any violation of critical safety conditions suppresses the entire reward.

A.3 Implementation details

Architecture. We use a discrete motion token vocabulary of size 1024 for each agent category (Vehicle, Pedestrian, Cyclist), where each token corresponds to a 0.5-second movement segment. The ego agent shares the same token vocabulary as other vehicles in the Vehicle category. Our model adopts a 6-layer Transformer decoder, each with 8 attention heads and a hidden dimension of 128. At the end of each decoder layer, a token prediction head is applied, implemented as a two-layer MLP. The parameters of an autoregressive decoder are approximately 5.05M.

Training. During pretraining, we use teacher forcing to optimize next motion token prediction with cross-entropy loss. The model is trained for 32 epochs with a batch size of 64 using the AdamW optimizer [19], with a learning rate of 3×10^{-4} and a weight decay of 1×10^{-4} . A dropout rate of 0.1 is applied throughout training. A cosine annealing scheduler is used to decay the learning rate to zero during pretraining. For fine-tuning, we apply GRPO with a group size of $G = 4$, KL divergence regularization weight $\beta = 0.1$, and a reduced learning rate of 4×10^{-5} . Fine-tuning is performed for 5 epochs, using the same dropout rate of 0.1 as in pretraining. No data augmentation is applied during either training or fine-tuning. All experiments are conducted on 8 NVIDIA RTX 4090 GPUs.

Simulation. During simulation, both the pretrained and fine-tuned models generate trajectories by selecting the top-1 token at each step.

A.4 Limitations and future work

The fine-tuning stage of our method relies on a set of rule-based rewards, whose design and weight calibration require substantial manual effort and iterative tuning. Furthermore, the fine-tuning process depends on trajectories sampled from the pretrained model, which may fail to capture rare yet critical behavior, such as emergency braking to avoid collisions, due to their limited presence in expert demonstrations. As part of future work, we plan to collect a set of safety-critical scenarios and apply supervised fine-tuning (SFT) to provide a stronger initialization prior to reinforcement learning.

A.5 Broader impacts

This work introduces a novel perspective on trajectory planning by framing it as a principle-aligned autoregressive generation task. By decoupling behavior learning from planning principle alignment, our approach facilitates the generation of safer and more feasible trajectories in complex driving scenarios. The proposed framework has the potential to advance the development of more reliable planning systems for autonomous vehicles and may contribute to enhancing safety in both simulation and real-world applications. This research is intended solely for academic and simulation-based

exploration. No deployable system is released. Any real-world deployment would require extensive additional testing, regulatory oversight, real-world validation, and continuous safety monitoring to ensure responsible use.